Evidence for a Quadrupolar Excitation Channel at the L_{III} Edge of Gadolinium by Resonant Inelastic X-Ray Scattering

M. H. Krisch,[1] C. C. Kao,[2] F. Sette,[1] W. A. Caliebe,[2] K. Hämäläinen,[3] and J. B. Hastings[2]

[1]*European Synchrotron Radiation Facility, F-38043 Granoble Cedex, France*

[2]*National Synchrotron Light Source, Brookhaven National Laboratory, Upton, New York 11973*

[3]*Department of Physics, University of Helsinki, Siltavuorenpenger 20D, SF-00170 Helsinki, Finland*

(Received 2 December 1994)

The weak $2p^5 4f^{n+1}$ quadrupolar excitation is separated from the intense $2p^5 5d^1$ white line at the gadolinium L_{III} absorption edge in $Gd_3Ga_5O_{12}$ by resonant inelastic x-ray scattering. This separation is obtained monitoring the intensity of the $3d^9 4f^{n+1} 5d^0$ and $3d^9 4f^n 5d^1$ multiplet families, which are resonantly enhanced at the $2p^5 4f^{n+1}$ and $2p^5 5d^1$ intermediate excitation energies, respectively. The dipolar and quadrupolar excitations are detected in spite of the Gd $2p$ lifetime broadening, thanks to the large Coulomb energy difference between the $3d^9 4f^{n+1} 5d^0$ and $3d^9 4f^n 5d^1$ multiplet families.

PACS numbers: 75.25.+z, 75.50.Bb, 75.50.Cc, 78.70.Dm

The study of near-edge resonance in x-ray absorption spectra has been widely utilized to obtain information on the local electronic structure around the excited atom. Strong resonances are often observed and generally attributed to dipole allowed core excitations in the lowest energy empty states. Weak preedge features are observed as well and, in some cases, assigned to quadrupolar excitations. An experimental method for their firm assignment, however, is still lacking, although there are important cases where this knowledge is necessary for the proper data interpretation. One example is the dipolar or quadrupolar origin of the feature typically observed below the L_{III} absorption edges in x-ray magnetic circular dichroism (XMCD) studies of rare-earth elements and compounds [1–9]. The assignment is of primary importance in comparing the experimental data with spin-dependent electronic structure calculations and in applying the novel magneto-optical sum rules to derive important ground state quantities, such as the atomic orbital and spin magnetic mements [10,11]. A prototypical case is represented by the XMCD at the gadolinium L_{III} edge, where the XMCD feature below the edge cannot be related to any corresponding feature in the absorptoin spectrum, either because of the $2p$ core-hole lifetime broadening or because of the very different intensity contributions to the white line expected from the $2p \rightarrow 4f$ quadrupolar ($E2$) and $2p \rightarrow 5d$ dipolar ($E1$) transitions.

In this Letter we show that it is possible to resolve the $E1$ and $E2$ excitation channels in gadolinium using resonant inelastic x-ray scattering [12]. This is accomplished by measuring the inelastic scattering spectra associated with the $3d^9 4f^{n+1} 5d^0$ and $3d^9 4f^n 5d^1$ final states. These two final states are two multiplet families, separated in energy by approximately 8 eV as a result of their different Coulomb integrals, and are characterized by a width determined by the $3d$ core-hole lifetime broadening and its multiplets splittings. When the incident photon energy $\hbar\omega_1$ is tuned through the L_{III} absorption edge, the inelastic scattering cross sections from the $3d^9 4f^{n+1} 5d^0$ and $3d^9 4f^n 5d^1$ final states are resonantly enhanced at the $2p^5 4f^{n+1} 5d^0$ quadrupolar and $2p^5 4f^n 5d^1$ dipolar excitation energies, respectively. The study of the intensity of these two multiplet families as a function of the incident photon energy allows the separation of the two excitation channels, in spite of the $2p$ core-hole lifetime broadening and the very different intensity contributions of the two channels to the white line. More generally, this new approach to near-edge x-ray absorption spectroscopy can be used to separate overlapping bound states in the absorption spectra as long as these excitation channels decay into final states which are sufficiently separated in the corresponding inelastic x-ray scattering spectra.

The experiment was performed at the wiggler beam line X21 at the National Synchrotron Light Source. The experimental configuration consists of two focusing Rowland circle geometries in the horizontal scattering plane. The incoming radiation from a 27 pole wiggler is monochromatized by a cylindrically bent, asymmetrically cut silicon (220) crystal. The monochromator provides a 1 mm horizontal and 10 mm vertical line focused beam, linearly polarized in the horizontal plane, and has an energy resolution of 0.6 eV full width at half maximum (FWHM). The sample used in the experiment was a $Gd_3Ga_5O_{12}$ garnet (GGG), positioned at the line focus of the monochromator. The scattered radiation was analyzed at a 90° scattering angle in the horizontal plane by a spherically bent silicon (333) crystal. In this geometry, due to the polarization factor, the contribution from the nonresonant Thomson scattering term in the interaction Hamiltonian is minimized with respect to the resonant $\mathbf{p} \cdot \mathbf{A}$ term and can be neglected. At incident photon energeis around the L_{III} absorption edge, the incident flux on the sample was 2×10^{11} photons/sec (at 100 mA ring current) and the overall experimental resolution was 1.3 eV FWHM.

Figure 1 shows the Gd^{3+} L_{III} x-ray absorption spectrum measured from a thin GGG sample. The spectrum, essentially identical to that of the Gd metal [1], shows a

0031-9007/95/74(24)/4931(4)$06.00

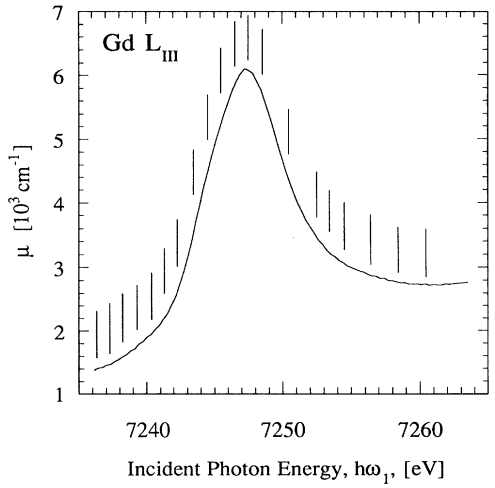

FIG. 1. Absorption coefficient of Gd in GGG around the L_{III} edge of Gd. The vertical lines correspond to the incident photon energies at which the high resolution spectra of the inelastically scattered photons were measured.

single white line dominated by the strong dipole allowed $2p$ to $5d$ dipolar transition. The absorption coefficient was obtained by normalizing the measured intensity well below and above the edge to the corresponding values calculated for the Gd atom [13]. The absorption edge energy is taken at the first inflection point in the absorption spectrum and is located at 7243 ± 2 eV. Although the energy resolution used in this measurement is 0.6 eV, no other spectral feature is observed due to the large natural lifetime width of the $2p$ core hole of about 4 eV. The vertical lines in the figure correspond to the incident photon energeis $\hbar\omega_1$, at which the high resolution spectra of the inelastically scattered photons of energy $\hbar\omega_2$ were measured.

Representative normalized inelastic scattering spectra are shown in Fig. 2. The scattered intensity is plotted as a function of energy transfer to the sample $\hbar\omega_1 - \hbar\omega_2$, which corresponds to the excitation energy of the different final state multiplet families with respect to the ground state. The observed structures in these spectra can be divided into three groups, labeled A, B, and C. Group A centers at 1180.7 eV, with its intensity going through a maximum at 7240 eV. Group B centers at 1188.6 eV and goes through a maximum at 7247.5 eV. There is also a gradual shift of the peak position from 1188.6 to 1190 eV. The shoulder, indicated as B*, follows the evolution of peak B, as will be clearer later on. It is therefore assigned to be part of the same multiplet family as peak B. Peak C starts to grow at 7250.5 eV incident photon energy between peaks B and B*, and its energy value increases with increasing incident energy.

These features, as can be seen in the bottom curves of Fig. 2, have decreasing intensity below the L_{III} edge and can no longer be observed at $\hbar\omega_1$ values well below

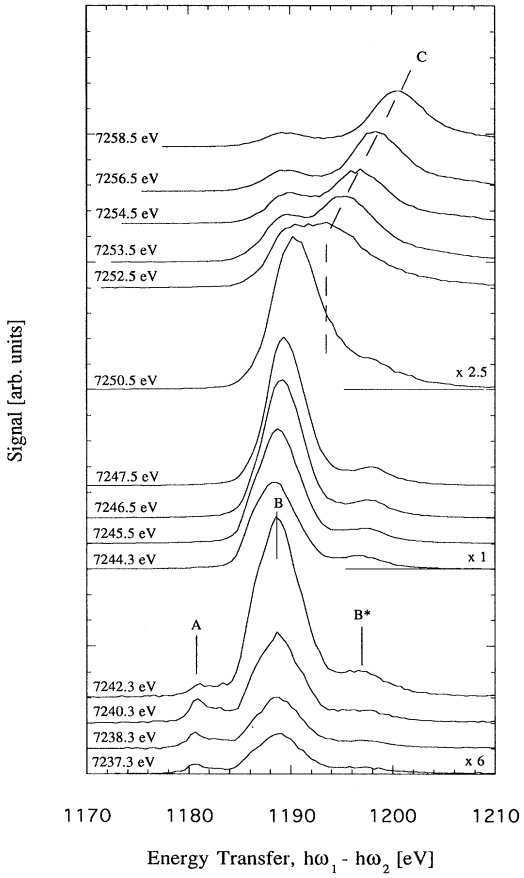

FIG. 2. Inelastic scattering spectra from GGG. The incident photon energy at which the spectra are taken is given in the figure. The spectra are corrected for self-absorption effects. They are divided into three groups labeled by the corresponding scaling factor. The dashed line is a guide to the eye used to show the behavior of the fluorescent line C, increasing in intensity below the continuum threshold where it stays at constant energy transfer, and with almost constant intensity above threshold where it shifts continuously with energy transfer.

the L_{III} edge energy. This indicates that they are all associated with second-order resonant inelastic scattering from the $\mathbf{p} \cdot \mathbf{A}$ term in the interaction Hamiltonian and that the dominating intermediate virtual states have a core hole in the $2p$ level. In particular, the behavior of peak C is typical of excitations into continuum states, where the scattered radiation above threshold is always observed at fixed $\hbar\omega_2$, which in this case corresponds to the $L\alpha_1$ fluorscence energy (6058 ± 1 eV). On the contrary, the behavior of peaks A and B shows the presence of two different resonances inside the L_{III} white line. The intensity of peaks A and B reaches maximum at $\hbar\omega_1 = 7240$ and 7247.5 eV, respectively; their integrated intensity values as a function of $\hbar\omega_1$ follow the Lorentzian decay of the $2p$ core-hole linewidth.

To demonstrate even more directly the presence of these two resonances in the white line, to determine their relative strength, and to investigate the origin of the feature B*, we scanned the incident energy $\hbar\omega_1$ and the scattered energy $\hbar\omega_2$ together, thus keeping the energy transfer constant. The results of these combined scans are displayed in Fig. 3, where the curves were taken at the following energy transfers: 1180.7, 1188.6, and 1196.7 eV. To follow the maximum intensity of feature C, the spectrometer is kept at fixed $\hbar\omega_2 = 6058$ eV above 7255 eV. From Fig. 3, it is evident that curves A and B correspond to two different resonances, with full width at half maxima of 4.7 and 5.8 eV, respectively. This value compares well with the $2p$ core-hole lifetime width. The maximum intensity of peak A is only $\sim 1.8\%$ of that of peak B. We also see that feature B* shows the same behavior as feature B, confirming that it belongs to the same multiplet family.

Group A is assigned to the multiplet family corresponding to the $3d^9 4f^{n+1} 5d^0$ final state of the Gd^{3+} ion. Group B is assigned to the $3d^9 4f^n 5d^1$ final states and group C to the $3d^9 4f^n 5d^0 \varepsilon^*$ continuum state. This assignment is consistent with the role played by the electron promoted into the different empty states: In particular, an extra electron in the localized $4f$ orbitals has a larger Coulomb interaction with the $3d$ core hole, making a more tightly bound final state in comparison to an electron promoted either to the $5d$ orbital or to the continuum. Consequently, the excitation energy is smaller for the $3d^9 4f^{n+1} 5d^0$ final state than that for the $3d^9 4f^n 5d^1$ and $3d^9 4f^n 5d^1 \varepsilon^*$ final states.

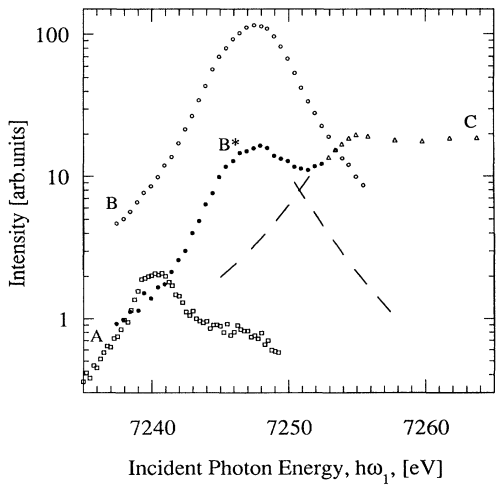

FIG. 3. Constant energy transfer scans for three different energy transfers: feature A (cubes), 1180.7 eV; feature B (open circles), 1188.6 eV; and feature B* (closed circles), 1196.7 eV. The spectrum labeled C (triangles) is taken at constant energy $\hbar\omega_2$. The spectra are corrected for self-absorption effects. The dashed lines are guides to the eye used to show the resonant behavior of feature B* and the behavior of the fluorescent line C, increasing in intensity below the continuum threshold, and with constant intensity above threshold.

The assignment of group A is further confirmed by the resemblance of its line shape to that of its direct analog in the Gd^{3+} M_V near-edge absorption spectrum [14]. The near-edge resonance in the M_V absorption spectrum is, in fact, characterized by the same $3d^9 4f^{n+1} 5d^0$ final state and, indeed, shows the same double peak structure seen in group A. Finally, as noted before, features B and B* in Fig. 2 show an energy shift with increasing incident energy. This behavior can be accounted for by two multiplet families separated by ~ 1.3 eV, which resonate at slightly different incident photon energies. This separation could be related to the exchange splitting of the $5d$ band, which is expected to be of this order of magnitude [15].

The analysis of Figs. 2 and 3 shows that the *central ingredient* which allows the separation among different excitation channels contributing to the same near-edge absorption resonance is the *comparison* of the *lifetime broadening of the final state* (the $3d$ core-hole lifetime in our case, and not the much wider $2p$ core-hole lifetime of the intermediate state) with the *energy separation among the multiplet families* generated by the decay of the overlapping excitation channels. In the resonant inelastic scattering spectrum, in fact, these multiplet families can be separated as long as their energy difference is *larger* than the final state core-hole lifetime broadening. Once this condition is fulfilled, one can immediately generate the results shown in Fig. 3, where the relative contribution to the absorption spectrum of overlapping channels is completely resolved, in spite of the $2p$ core-hole lifetime broadening and of possible large differences in relative intensities.

We now discuss our resonant inelastic scattering results in relation to the question of the origin of the XMCD feature below the L_{III} absorption edge of Gd. As we have seen, the white line at the Gd L_{III} edge has contributions from the $2p^5 4f^{n+1} 5d^0$ and $2p^5 4f^n 5d^1$ excitations. The energies of these excitations are at -3 and 4.5 eV with respect to the absorption edge (maximum intensity of groups A and B in Fig. 3). The energy position of the excitation decaying into the group A multiplet is essentially the same as the negative feature in the L_{III} Gd XMCD spectrum. At this energy, the contribution of group A to the total absorption cross section is about 18%, while that from group B is about 82%. Although the exact ratio in the case of Gd metal may be slightly different from the number obtained here for the Gd^{3+} ion, it is clear from our data that the XMCD feature below the Gd L_{III} absorption edge must have a contribution from both the $E1$ and the $E2$ transitions. Considering that the $E1$ transition gives a positive XMCD signal while the $E2$ transition gives a negative XMCD signal, there are strong grounds to conclude that the XMCD below the Gd L_{III} edge has a quadrupolar contribution. This is in agreement with theoretical predictions by Carra *et al.* [4]. Further angular dependent measurements [4,16] using circularly polarized x rays cannot help to clear up this point. The Gd^{3+} ion in fact, due to its $^8S_{7/2}$ ground state, gives an

angular dependence for the $E2$ XMCD very similar to that of $E1$.

In summary, our experimental method allows us to separate two different absorption channels with a relative intensity ratio of 50:1, which would be completely indistinguishable in a standard absorption measurement. This is accomplished by resonant inelastic x-ray scattering measurements, using the property that the considered final states, resulting from different decay channels of overlapping intermediate core-hole excitations, have a large energy separation with respect to the final state core-hole lifetime. Moreover, the features in the inelastic scattering spectra allow us to assign the final state to the $3d^9 4f^{n+1} 5d^0$ and $3d^9 4f^n 5d^1$ multiplet families and to assess, therefore, the existence and intensity of the quadrupolar $2p^5 4f^{n+1} 5d^0$ excitation in the Gd L_{III} white line.

More importantly, resonant inelastic x-ray scattering offers a unique way to measure the near-edge absorption spectra by selectively probing the particular intermediate state (or states) that decay into the final state which is monitored. It should also be noted that, through the intermediate state, the inelastic scattering spectra can also include dipole forbidden transitions, such as the $3d$ to $5d$ transition in Gd, corresponding to the $3d^9 4f^n 5d^1$ final state.

Finally, resonant inelastic x-ray scattering excited with circularly polarized x rays will provide a new way to measure XMCD spectra with increased selectivity.

We acknowledge useful discussions with P. Carra and J. Goulon. The National Synchrotron Light Source is supported by the U.S. Department of Energy under Contract No. DE-ACO2-76CH00016.

[1] G. Schütz, M. Knülle, R. Wienke, W. Wilhelm, W. Wagner, P. Kienle, and R. Frahm, Z. Phys. B **73**, 67 (1988).
[2] P. Fischer, G. Schütz, S. Stähler, and G. Wiesinger, J. Appl. Phys. **69**, 6144 (1991).
[3] P. Carra and M. Altarelli, Phys. Rev. Lett. **64**, 1286 (1990).
[4] P. Carra, B. N. Harmon, B. T. Thole, M. Altarelli, and G. A. Sawatzky, Phys. Rev. Lett. **66**, 2495 (1991).
[5] J. C. Lang, S. W. Kycia, X. D. Wang, B. N. Harmon, A. I. Goldman, D. J. Branagan, R. W. McCallum, and K. D. Finkelstein, Phys. Rev. B **46**, 5298 (1992).
[6] X. Wang, T. C. Leung, B. N. Harmon, and P. Carra, Phys. Rev. B **47**, 9087 (1993).
[7] K. Shimomi, H. Maruyama, K. Kobayashi, A. Koizumi, H. Yamazaki, and T. Iwazumi, Jpn. J. Appl. Phys. **32**, Suppl. 32–2, 314 (1993).
[8] H. Maruyama *et al.*, J. Phys. Soc. Jpn. **60**, 1456 (1991).
[9] F. Baudelet, C. Brouder, E. Dartyge, A. Fontaine, J. P. Kappler, and G. Krill, J. Magn. Magn. Mater. **104–107**, 1418 (1992).
[10] B. T. Thole, P. Carra, F. Sette, and G. van der Laan, Phys. Rev. Lett. **68**, 1943 (1992).
[11] P. Carra, B. T. Thole, M. Altarelli, and X. Wang, Phys. Rev. Lett. **70**, 694 (1993).
[12] T. Åberg and J. Tulkki, in *Atomic Inner-Shell Physics*, edited by B. Crasemann (Plenum, New York, 1985).
[13] D. T. Cromer and D. Liberman, J. Chem. Phys. **53**, 1891 (1970).
[14] J. Goedkoop, thesis, University of Nijmegen, 1989.
[15] B. N. Harmon and A. J. Freeman, Phys. Rev. B **10**, 1979 (1974).
[16] J. C. Lang, G. Srajer, C. Detlefs, A. I. Goldman, H. König, X. Wang, B. N. Harmon, and R. W. Callum, following Letter, Phys. Rev. Lett. **74**, 4935 (1995).